Spontaneous surface roughening induced by surface interactions between two compressible elastic films

Jayati Sarkar,[1] Vijay Shenoy,[2] and Ashutosh Sharma[1,*]
[1]*Department of Chemical Engineering, Indian Institute of Technology, Kanpur, UP 208 016, India*
[2]*Materials Research Centre, IISc, Bangalore 560 012, India*
(Received 29 July 2002; published 25 March 2003)

The surfaces of soft thin elastic films bonded to two rigid substrates become spontaneously rough due to the attractive intersurface interactions when the intersurface distance declines sufficiently to produce a critical force. The effects of compressibility on the conditions for surface roughening and its length scale are investigated. For highly compressible films (ν less than 0.25), surface roughening is not possible. The critical force required for the onset of instability and its wave number both decline with increased compressibility. The wavelength of the instability is influenced much more by the properties of the more compliant film [compliance equals $(1-2\nu)h/2\mu(1-\nu)$]. There is an abrupt change in the wavelength as the compliances of the two films become nearly equal.

DOI: 10.1103/PhysRevE.67.031607 PACS number(s): 68.15.+e, 68.35.Ct, 68.55.−a, 46.50.+a

I. INTRODUCTION

Surfaces of soft thin elastic films undergo spontaneous roughening when brought in close contact proximity to another surface [1,2]. The surface instability is engendered by the attractive intersurface forces, for example, van der Waals and electrostatic forces, when the force exceeds a threshhold value [3,4]. The surface roughness thus spontaneously produced plays an important role in the understanding of contact mechanics, friction, and adhesion at soft interfaces. Some recent experiments [1,2,5] show that in contrast to the liquid films [6–9] where the length scale and morphology of the instability depend very strongly on the precise nature and magnitude of the interactions, the periodic wavelength that develops in thin solid elastic films is largely independent of the nature and magnitude of such interactions. Moreover, the wavelength depends almost linearly on the thicknesses of the films.

The surface instability of elastic films in proximity to a contactor occurs due to the interplay of the interaction energy, which tries to deform the film surface, and the elastic energy which tries to restore the initial configuration [3,4]. The origin and nature of this purely elastic instability is different from the roughening of solid films [10–13], where either surface diffusion, viscoelasticity or plasticity of the films play the dominant role.

The instability causes the surfaces of the films to jump in contact in a periodic way [1,2], thus forming nanoscale cavities. This phenomenon has an intimate relationship with the formation of type-I cracks [14] as the sufaces are pulled apart [2]. A related problem of debonding by chain pullout has also received attention [15].

Some applications such as the peeling of adhesives [16], wafer debonding [17], adhesion of cells to coated substrates involve two interacting elastic layers. The contact between metal surfaces carrying thin oxide layers is another example where spontaneous surface roughening has been observed recently [18].

The stability and pattern formation have been studied recently for incompressible films [19,20]. The objective of this paper is to explore the effects of compressibility on the stability and bifurcation behavior of the two-film system. Among other things, we show that the length scale of surface roughening increases with increased compressibility and the instability is absent in highly compressible materials that can simply jump into contact uniformly. Also, the wavelength of instability is governed to a greater extent by the more compressible film. The results obtained here are of relevance in the design and interpretation of important experiments on the adhesion instability and crack formation in these systems.

II. MODEL DESCRIPTION

The schematic diagram of two thin elastic films interacting with each other is shown in Fig. 1. The elastic films are bonded rigidly to a substrate and a contactor, forming a substrate-contactor system, each with its own film. The substrate film is called film a and its properties such as thickness, shear modulus, and Poisson's ratio are denoted by h_a, μ_a, and ν_a, respectively. Similarly, the contactor film is called film b and its properties are denoted by the material properties with the subscript b. (The elastomeric films may widely differ from each other in their physical properties.) The separation distance between the two films is denoted by d_0. Below a certain critical separation distance d_c the films no longer remain planar, but a surface instability sets in, making the surfaces rough. The broken lines in Fig. 1 show periodic surface roughening under such circumstances. The length of each film along the depth of the paper is assumed to be much larger than the other lateral dimensions, so the system is considered to be undergoing plane strain deformations. The total potential energy of the deformed films (neglecting surface energy effects) is given by a sum of the stored elastic energy and the energy due to intersurface interactions [3],

*Author to whom correspondence should be addressed. Email address: ashutos@iitk.ac.in

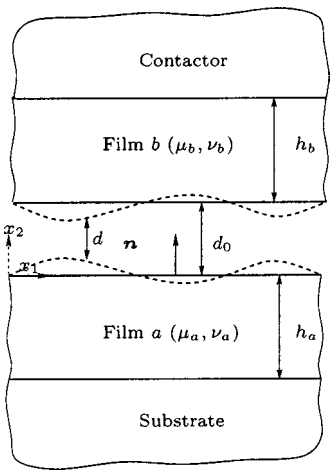

FIG. 1. A thin elastic film bonded to a rigid substrate interacting with a second film bonded to a contactor. The coordinate system (x_1, x_2) is used to describe the position vectors. (Distances are not to scale. The gap distance is largely exaggerated and the dashed lines indicate the initial stages of roughening.)

$$\Pi = \int_V W(\boldsymbol{\epsilon}) dV + \int_S U(d) dS, \tag{1}$$

where $\boldsymbol{\epsilon}$ is the strain tensor and W is the strain energy density given by the following expression:

$$W(\boldsymbol{\epsilon}) = \begin{cases} \mu_a \left(\boldsymbol{\epsilon} : \boldsymbol{\epsilon} + \dfrac{\nu_a}{1-2\nu_a} (\mathrm{tr}\, \boldsymbol{\epsilon})^2 \right) & \text{in film } a, \\ \mu_b \left(\boldsymbol{\epsilon} : \boldsymbol{\epsilon} + \dfrac{\nu_b}{1-2\nu_b} (\mathrm{tr}\, \boldsymbol{\epsilon})^2 \right) & \text{in film } b. \end{cases} \tag{2}$$

The term under the surface integral in Eq. (1) arises due to the attractive interaction potential that exists between the two films. The attractive potential U is the excess free energy of interactions per unit area, which may be due to van der Waals forces, electrostatic forces, etc., and is a function of the intersurface distance d. The form of the potential may be simply van der Waals (3), or an extended form given by Eq. (4):

$$U(d) = -\frac{A}{12\pi d^2}, \tag{3}$$

$$U(d) = -\frac{A}{12\pi d^2} + \frac{B}{d^8} + S \exp\left[\frac{d_e - d}{l_p} \right], \tag{4}$$

where

$$d = d_0 - (\boldsymbol{u}^a - \boldsymbol{u}^b) \cdot \boldsymbol{n} \tag{5}$$

is the effective separation distance that remains between the two films when they undergo a displacement of $\boldsymbol{u}^a$ and $\boldsymbol{u}^b$, respectively, from their undeformed separation d_0. The first term in the potential comes from the attractive van der Waals interaction, where A is the Hamaker constant (of the order of 10^{-19} J). The second term arises due to Born repulsion and the third term introduces a short range non–van der Waals attraction $(S<0)$ close to contact with a decay length l_p. This term also incorporates the non–van der Waals component of the free energy of adhesion. The constants B and S in Eq. (4) are of the order of 10^{-74} J m^6 and -0.1 J/m^2, respectively, and their exact values are obtained by imposing the following conditions at the equilibrium separation distance d_e, taken to be 1 nm in the present analysis:

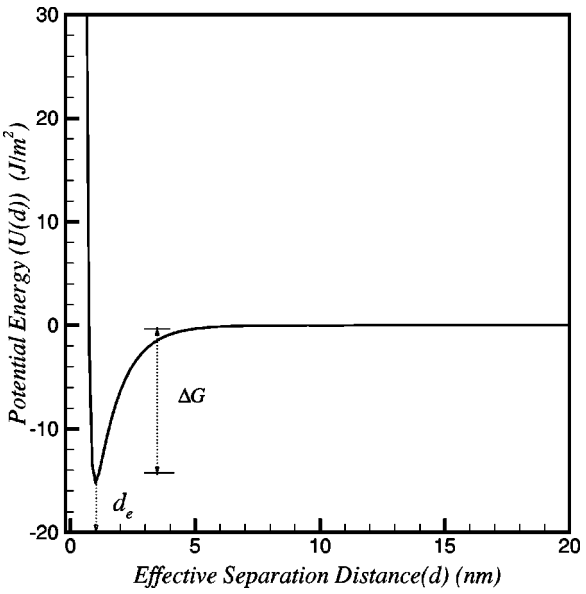

FIG. 2. Schematic of the potential under consideration. The equilibrium distance is denoted by d_e.

$$U'(d_e) = 0,$$

$$U(d_e) = \Delta G = \text{total energy of adhesion.} \tag{6}$$

A sketch of the potential is shown in Fig. 2. As is known previously for a single film [3], and as will also be shown subsequently in this paper, neither the precise functional form of the potential, nor the precise values of the parameters in the potential, are of significance since the wavelength of instability is independent of the nature of interactions. The details of the potential affect only the critical separation distance for the onset of instability.

In order to carry out a linear stability analysis, the potential is expanded in a power series about the reference state of the undeformed films $d = d_0$ and the terms up to the quadratic order in $(\boldsymbol{u}^a - \boldsymbol{u}^b) \cdot \boldsymbol{n}$ are retained [see Eq. (4)],

$$U(d) \approx U_0 + F(\boldsymbol{u}^a - \boldsymbol{u}^b) \cdot \boldsymbol{n} + \frac{1}{2} Y [(\boldsymbol{u}^a - \boldsymbol{u}^b) \cdot \boldsymbol{n}]^2, \tag{7}$$

where

$$U_0 = U(d_0), \quad F = U'(d_0), \quad Y = U''(d_0). \tag{8}$$

The form Y is of the form (9) or (10) depending on the form of the potential (3) or (4),

$$Y=-\frac{A}{2\pi d_0^4}, \tag{9}$$

$$Y=-\frac{A}{2\pi d_0^4}+\frac{72}{d_0^{10}}\frac{[A(1-d_e/2l_p)/6\pi d_e^3-\Delta G/l_p]d_e^9}{(8-d_e/l_p)} + \frac{(8\Delta G+A/2\pi d_e^2)}{l_p^2(8-d_e/l_p)}\exp\left(\frac{d_e-d_0}{l_p}\right). \tag{10}$$

From the above equation it is clear that with decreasing initial gap thickness d_0, the magnitude of Y increases in the attractive regime of the potential. The dimensions of Y suggest that it is force per unit volume and is termed the *interaction stiffness*, and it is of importance in that it governs the condition for the onset of instability (below a critical separation distance the magnitude of Y, or the attractive force increases beyond a threshold value to initiate instabilities in the system). Similarly, F is the force per unit area. The above linearization gives an expression for the total potential energy as

$$\Pi_a=\int_V W(\boldsymbol{\epsilon})dV+\int_S\left[U_0+F(\boldsymbol{u}^a-\boldsymbol{u}^b)\cdot\boldsymbol{n} + \frac{1}{2}Y((\boldsymbol{u}^a-\boldsymbol{u}^b)\cdot\boldsymbol{n})^2\right]dS. \tag{11}$$

The equilibrium displacement fields in the films minimize the potential energy (11) while satisfying the following boundary conditions.

(1) Rigid boundary condition:

$$\boldsymbol{u}^a(x_1,-h_a)=0, \tag{12}$$

$$\boldsymbol{u}^b(x_1,d_0+h_b)=0, \tag{13}$$

i.e., the substrate and the contactor films are rigidly held at the film-substrate and the film-contactor interface.

(2) Traction boundary condition: The stresses derived from the displacement fields must satisfy the condition of vanishing shear stress at the interface, i.e.,

$$\sigma_{12}^a(x_1,0)=0, \tag{14}$$

$$\sigma_{12}^b(x_1,d_0)=0, \tag{15}$$

and the normal stresses satisfy the condition

$$\sigma_{22}^a(x_1,0)=-\{F+Y[u_2^a(x_1,0)-u_2^b(x_2,d_0)]\}, \tag{16}$$

$$\sigma_{22}^b(x_1,d_0)=-\{F+Y[u_2^a(x_1,0)-u_2^b(x_2,d_0)]\} \tag{17}$$

at respective surfaces.

Homogeneous solution. The boundary value problem defined by the above set of equations for compressible films has a homogeneous solution denoted by $\boldsymbol{u}^h$ such that the stresses in the films are everywhere equal. Thus, u_2^h denotes a uniform increase in the film thickness,

$$u_1^{ah}(x_1,x_2)=0,$$

$$u_1^{bh}(x_1,x_2)=0,$$

$$u_2^{ah}(x_1,x_2)=-\frac{1}{Y_m^a}\{F+Y[u_2^{ah}(x_1,0)-u_2^{bh}(x_2,d_0)]\}\left(1+\frac{x_2}{h_a}\right),$$

$$u_2^{bh}(x_1,x_2)=-\frac{1}{Y_m^b}\{F+Y[u_2^{ah}(x_1,0)-u_2^{bh}(x_2,d_0)]\}\times\left(\frac{x_2}{h_b}-1-\frac{d_0}{h_b}\right), \tag{18}$$

where

$$Y_m^a=\frac{2\mu_a(1-\nu_a)}{(1-2\nu_a)h_a}, \tag{19}$$

$$Y_m^b=\frac{2\mu_b(1-\nu_b)}{(1-2\nu_b)h_b}. \tag{20}$$

The homogeneous solution indicates that for compressible films the surface of both the films will move towards each other by an amount U^h given by

$$U^h=\frac{(-F)}{Y_m-(-Y)}, \tag{21}$$

where Y_m for the system is given by

$$Y_m=\frac{Y_m^aY_m^b}{Y_m^a+Y_m^b}. \tag{22}$$

From this relation it is evident that the homogeneous solution is valid only when $-Y<Y_m$ ($-F$, $-Y$, and Y_m being positive quantities). For larger values of $-Y$, the film surfaces jump to make homogeneous contact with each other so that the films are everywhere in contact.

III. STABILITY ANALYSIS

The stability of the homogeneous state is evaluated by means of a linearized analysis. The homogeneous solution is perturbed by sinusoidal displacements. The bifurcation field in the films a and b takes the form

$$u_2^{ai}(x_1,0)=\alpha\cos(kx_1), \tag{23}$$

$$u_2^{bi}(x_1,d_0)=\beta\cos(kx_1), \tag{24}$$

respectively. Here i in the superscript denotes inhomogeneous solution. The *additional stresses* produced by these fields satisfy the rigid boundary conditions (12) and (13), vanishing shear stress conditions given by Eqs. (14) and (15), and the condition of normal traction

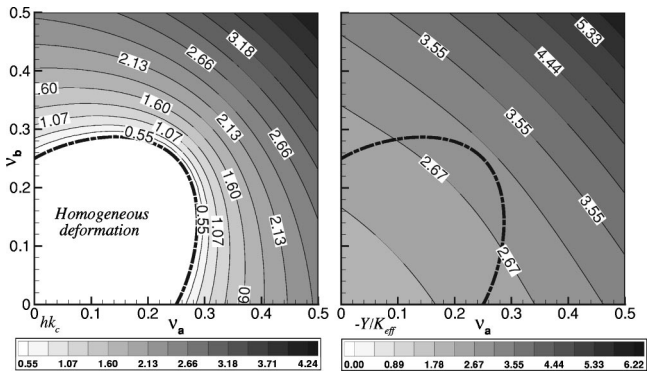

FIG. 3. Plots of the wave number of instability (hk_c) and the nondimensional critical interaction stiffness ($-Y_c/K_{eff}$) for a system with $H=0.5$ and $M=0.5$. The thick line in the diagrams shows the demarcation between regions of homogeneous and inhomogeneous deformations. In the region enclosed by the line, $hk_c=0$ and $-Y_c/K_{eff}$ takes the value of Y_m/K_{eff} for plots in the right column.

$$\sigma_{22}^{ai}(x_1,0) = -Y[u_2^{ai}(x_1,0) - u_2^{bi}(x_1,d_0)], \tag{25}$$

$$\sigma_{22}^{bi}(x_1,d_0) = -Y[u_2^{ai}(x_1,0) - u_2^{bi}(x_1,d_0)] \tag{26}$$

along the interacting surfaces of the films.

A film with sinusoidal displacement as given in Eq. (23) is shown in Appendix A to have stress σ_{22}^{ai} at the surface of the film as

$$\sigma_{22}^{ai}(x_1,0) = 2\mu^a S(h_a k,\nu_a) k\alpha \cos(kx_1). \tag{27}$$

Similarly, the stress $\sigma_{22}^{bi}(x_1,d_0)$ along the surface of the film b is

$$\sigma_{22}^{bi}(x_1,d_0) = -2\mu^b S(h_b k,\nu_b) k\beta \cos(kx_1), \tag{28}$$

where S is a nondimensional function defined as

$$S(\xi,\nu) = \frac{1+(3-4\nu)\cosh(2\xi)+2\xi^2+4(2\nu-1)(\nu-1)}{2(1-\nu)[(3-4\nu)\sinh(2\xi)-2\xi]}. \tag{29}$$

The stresses along the surface of the film must satisfy the normal traction condition. Thus substitution of Eqs. (27) and (28) in Eqs. (25) and (26) sets the condition for the existence of nontrivial bifurcation fields. It states that the interaction stiffness Y must be related to the physical parameters of the system along with the wave number k (of the bifurcation field) by the following expression:

$$Y = -\frac{2k\mu_a\mu_b S(h_a k,\nu_a) S(h_b k,\nu_b)}{\mu_a S(h_a k,\nu_a) + \mu_b S(h_b k,\nu_b)}. \tag{30}$$

If, for a given value of Y, i.e, for a given interaction stiffness, and a given separation distance there exists at least one real value of k that solves Eq. (30), then the homogeneous solution is unstable and the films deform inhomogeneously. The negative sign of Y indicates that the force is attractive in nature. The analysis is carried forth with $-Y$, denoting the magnitude of the interaction stiffness. The *lowest value* of

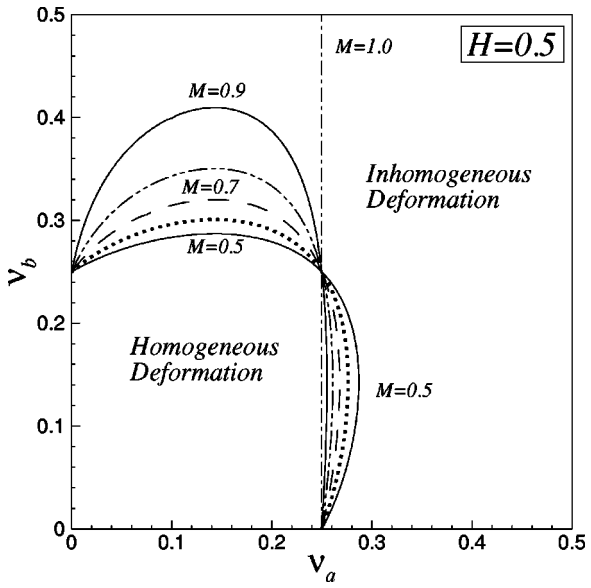

FIG. 4. Regions of homogeneous and inhomogeneous deformations in the space of Poisson's ratios of the films for different values of M. The films have equal thicknesses.

$-Y$ for which bifurcations are possible is called the *critical interaction stiffness* denoted by $-Y_c$. The wave number(s) of the mode(s) that satisfies (satisfy) Eq. (30) for $-Y=-Y_c$ is (are) called the critical mode(s) and the (these) wave number(s) is (are) denoted by k_c.

Apart from the Poisson's ratio, there are four parameters that enter the stability analysis, μ_a, μ_b, h_a, h_b and govern the stability of the film surfaces. The understanding of results is facilitated by defining certain effective parameters as motivated by the following analogy. Two interacting films can be visualized as two springs in series so that they undergo the same loading (tensile or compressive). In such cases it is seen that the total thickness of the system is the additive thickness and the effective elastic modulus is the harmonic mean of the individual modulus of the springs. From this analogy, we introduce the effective thickness and shear modulus of the system as

$$h = h_a + h_b, \tag{31}$$

$$\mu = \frac{\mu_a\mu_b}{\mu_a+\mu_b}. \tag{32}$$

Introduction of the following nondimensional parameters M and H further facilitates the investigation of the relative effects of the two films on the instability where

$$\frac{\mu}{\mu_a} = M, \quad \frac{\mu}{\mu_b} = (1-M) \tag{33}$$

and

$$h_a = Hh, \quad h_b = (1-H)h. \tag{34}$$

An important quantity of interest is the effective elastic stiffness K_{eff} of the two-film system defined as the harmonic mean of the individual stiffness of the films.

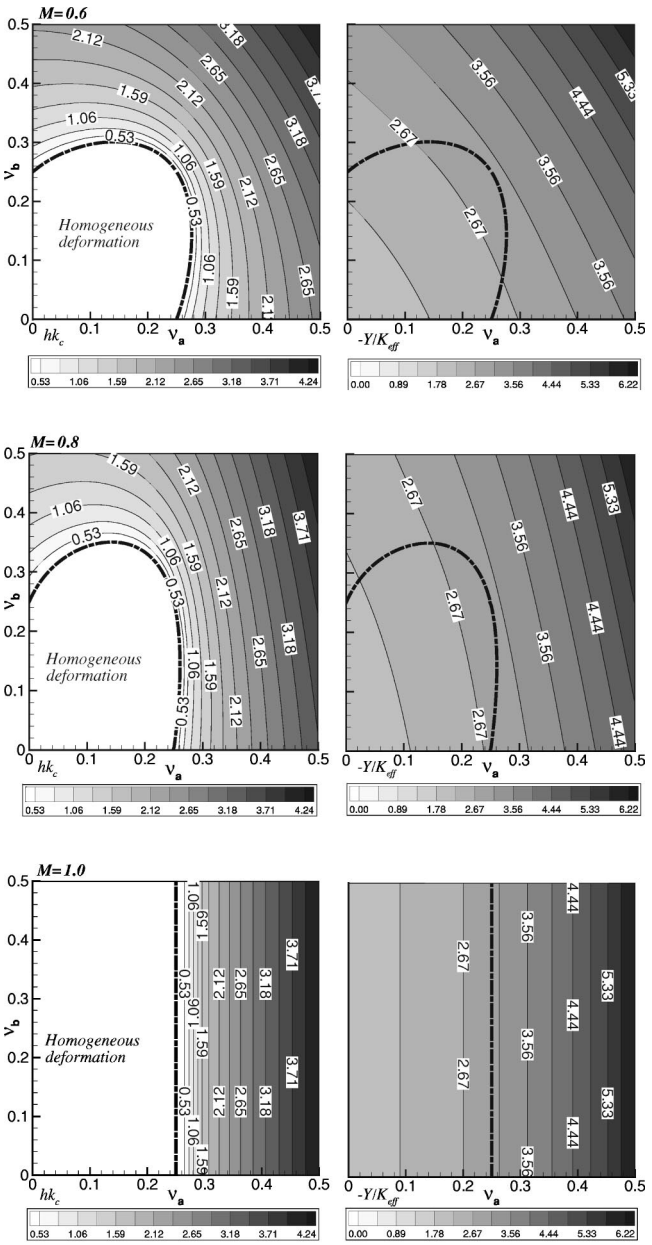

FIG. 5. Plots of the wave number of instability (hk_c) and the nondimensional critical interaction stiffness ($-Y_c/K_{eff}$) for different values of *M*, when the films have equal thicknesses. The thick line in the diagrams shows the demarcation between regions of homogeneous and inhomogeneous deformations. In the region enclosed by the line, $hk_c=0$ and $-Y_c/K_{eff}$ takes the value of Y_m/K_{eff} for plots in the right column.

$$K_{eff}=\frac{\dfrac{\mu_a}{h_a}\dfrac{\mu_b}{h_b}}{\dfrac{\mu_a}{h_a}+\dfrac{\mu_b}{h_b}}=\frac{\mu_a\mu_b}{\mu_a h_b+\mu_b h_a}$$

$$=\frac{\mu}{h}\frac{1}{[(1-H)(1-M)+HM]}. \tag{35}$$

Based on the above definitions, the expression for the interaction stiffness in Eq. (30) can be recast in the following nondimensional form:

$$\frac{-Y}{K_{eff}}=\frac{2[(1-H)(1-M)+HM]qS(Hq,\nu_a)S((1-H)q,\nu_b)}{(1-M)S(Hq,\nu_a)+MS((1-H)q,\nu_b)}, \tag{36}$$

where $q=hk$.

The stability conditions of an incompressible two-film model can be recovered by setting values of ν_a and ν_b to $\frac{1}{2}$ in Eq. (36). The other limiting cases of Eq. (36) can be obtained by setting $M\to 1$ and $H\to 1$.

The condition $M\to 1(\mu_b\gg\mu_a)$ implies that the contactor film is much more rigid compared to the substrate film and in view of this, the above equation transforms to

$$-\frac{Y}{K_{eff}}=2HqS(Hq,\nu_a)=2h_akS(h_ak,\nu_a), \tag{37}$$

which is the case of a compressible elastic film interacting with a rigid contactor. The other condition $H\to 1(h_a\gg h_b)$, implies that the thickness of the substrate film is much greater than the thickness of the contactor film. Equation (36) as $H\to 1$, transforms into

$$-\frac{Y}{K_{eff}}=\frac{2HqMS(Hq,\nu_a)}{(1-M)\dfrac{S(Hq,\nu_a)}{S((1-H)q,\nu_b)}+M}. \tag{38}$$

The condition $S(\xi,\nu)\to\infty$ as $\xi\to 0$, which when applied to Eq. (38) gives the same result as in Eq. (37), i.e, the case of a rigid contactor. Thus, it can be seen that the case of two incompressible films interacting with each other or the case of a single film interacting with a contactor are special cases of the present analysis.

IV. RESULTS AND DISCUSSIONS

The wave number of instability as found from Eq. (36) is dependent on the compressibility (Poisson's ratios) of the films and on the nondimensional parameters *M* and *H*, which can take values from 0 to 1. However, the symmetry of Eq. (36) in *M* and *H* allows to consider only the results in the regime $\frac{1}{2}\leqslant M\leqslant 1$ and $0\leqslant H\leqslant 1$. For each of these ranges of μ_a,μ_b and h_a,h_b, results are discussed for different values of ν_a and ν_b. In each case, the aim is to obtain regions in the (ν_a,ν_b) parameter space, where instability is possible (Figs. 4, 6, 8, and 9). In addition, the wave number of the instability and the critical interaction stiffness ($-Y_c/K_{eff}$) as a function of ν_a and ν_b (Figs. 3, 5, and 7) are also obtained.

To aid the discussion of the results of the two-film case, we recall here some of the observations of a single elastic film interacting with a rigid contactor given in Ref [4]. The wave number of instability (hk_c) and the critical interaction stiffness ($-Y_c$) of the film were found to decrease with an increase in compressibility of the film. Results for a single

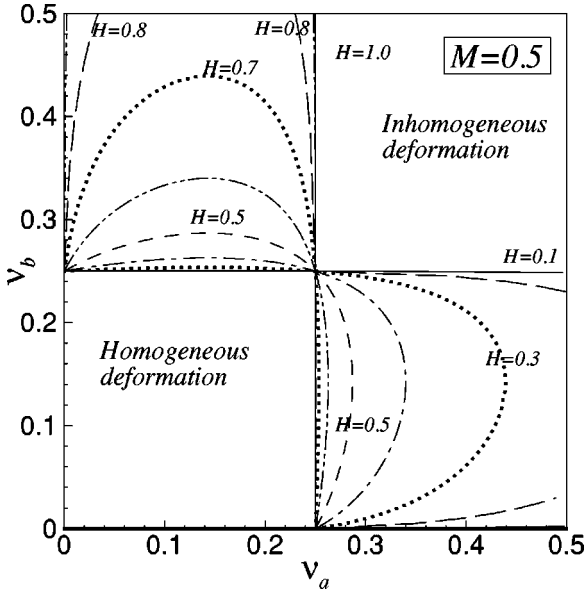

FIG. 6. Regions of homogeneous and inhomogeneous deformations in the space of Poisson's ratios of the films for different values of H. The films have equal shear moduli.

film are shown in Fig. 13. The physical significance of these observations is that it is energetically less expensive to produce elastic deformations in a compressible film. Thus the critical interaction stiffness $(-Y_c)$ required for inhomogeneous deformation is higher for an incompressible film than a compressible one. In addition, it is energetically favorable to produce near homogeneous deformations in a compressible film. Thus, the wavelength of instability $(\lambda_c = 2\pi/k_c)$ in a compressible film is higher than that of an incompressible film. The discussion for case of two films can also be based on energetic arguments. The relevant expression for the total energy of two films as a function of the shear modulus of the films and the dimensionless function S is shown in Appendix B.

A. Films with equal thicknesses and shear moduli

When the thicknesses and shear moduli of the two films are equal ($h_a = h_b$ and $\mu_a = \mu_b$), the nondimensional parameters H and M are both equal to $\frac{1}{2}$. In the bifurcation diagrams, Figs. 4 and 6, such a case is indicated by $M = 0.5$ and $H = 0.5$, respectively. It is seen that when the films have identical physical properties, the line demarcating the region of homogeneous and nonhomogeneous deformations is symmetric in the parametric space of ν_a and ν_b. The results in this case, for k_c and $-Y_c$ are shown in Fig. 3. If the Poisson's ratio of one film (say a) is kept fixed and the Poisson's ratio of the other film (ν_b) is decreased, the effective compressibility of the system increases. Similar to the one-film case, it is seen from Fig. 3 that $-Y_c/K_{eff}$ and hk_c values of the system decrease.

The effects of introducing the second film are illustrated for a system with $\nu_a = 0.35$ and $\nu_b = 0.45$. The wave number of instability of the system hk_c for this case is found to be 3.13 implying that the critical wavelength $(\lambda_c = 2\pi/k_c)$ at

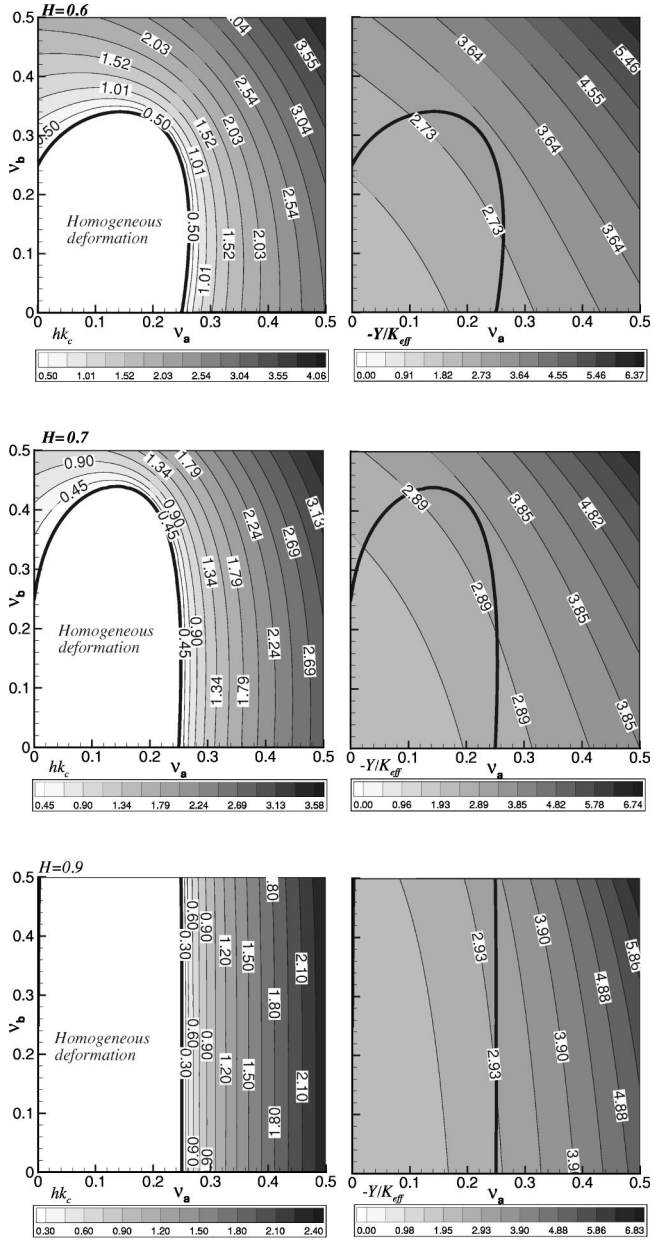

FIG. 7. Plots of the wave number of instability (hk_c) and the nondimensional critical interaction stiffness $(-Y_c/K_{eff})$ for a system with $M = 0.5$ and different values of H. The thick line in the diagrams shows the demarcation between regions of homogeneous and inhomogeneous deformations. In the region enclosed by the line, $hk_c = 0$ and $-Y_c/K_{eff}$ takes the value of Y_m/K_{eff} for plots in the right column.

this point is $4.01h_a$. For a single film interacting with a rigid contactor, the wavelength of instability for $\nu_a = 0.35$ and $\nu_a = 0.45$ is found from Appendix B to be $5.05h_a$ and $3.41h_a$, respectively. These results show that the wavelength of instability in the two-film system lies between the wavelengths of the two films had they been interacting with rigid contactors. For the same point in the parametric space, the value of the nondimensional interaction stiffness $-Y_c/K_{eff}$ is 4.56. For the present case, the effective stiffness of the system is given by $0.5\mu_a/h_a$, thus the value of the critical interaction

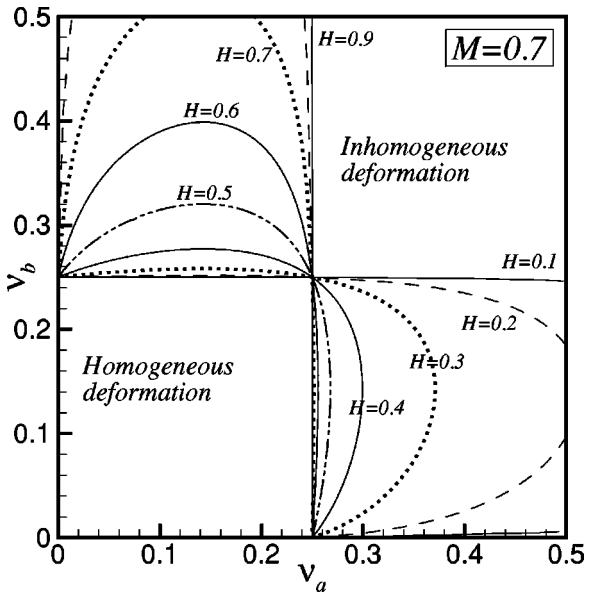

FIG. 8. Bifurcation zones as a function of the Poisson ratio and H when $M=0.7$.

stiffness is given as $-Y_c=2.28\mu_a/h_a$. From Appendix B, we see that for a film interacting with a rigid contactor, $-Y_c=3.08\mu_a/h_a$ for $\nu_a=0.35$ and $-Y_c=5.17\mu_a/h_a$ for $\nu_b=0.45$. This indicates that the critical interaction stiffness of the two-film system is lower than either of the interaction stiffnesses, had the films been interacting with rigid contactors. The results illustrate the fact that the introduction of a second film, in place of a rigid contactor, brings down the effective stiffness of the system, makes the system more compliant, and hence promotes instabilities in the system.

B. Films with equal thicknesses and different shear moduli

For the case when $H=0.5$, the regions of homogeneous and inhomogeneous deformations in the parametric space as

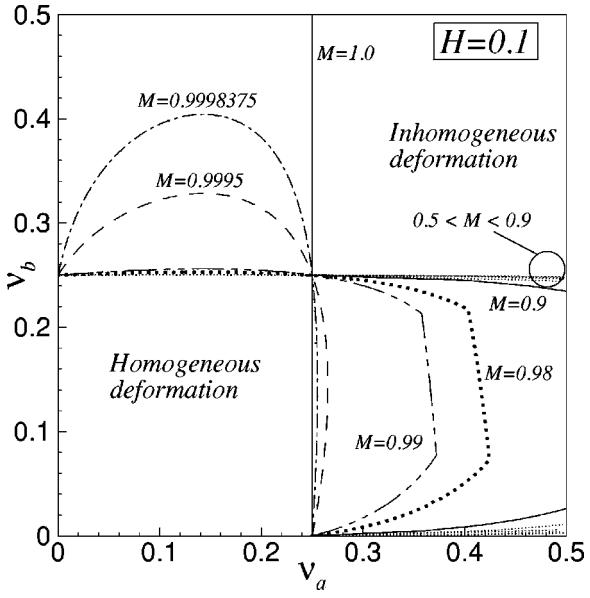

FIG. 9. Bifurcation zones as a function of the Poisson ratio and M when $H=0.1$.

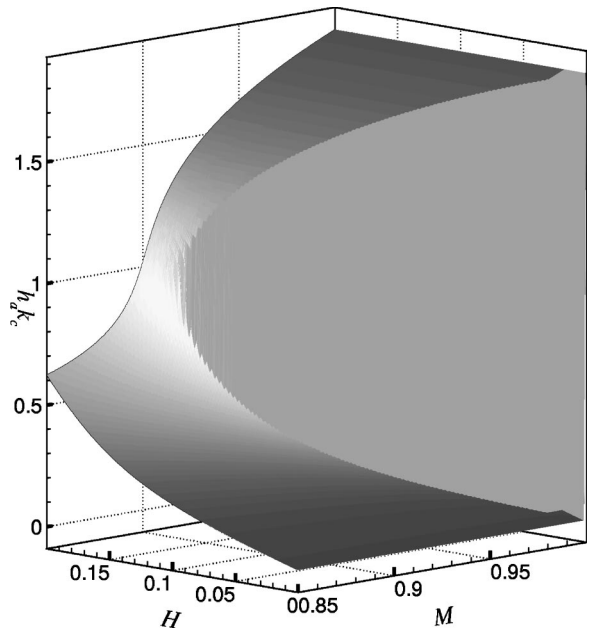

FIG. 10. The value of $h_a k_c$ as a function of H and M. The figure shows that above a certain value of M, the wave number shows a jump from a higher to a lower value for a particular value of H_J. The Poisson ratios of the films taken are $\nu_a=0.45$, $\nu_b=0.4$.

a function of the nondimensional parameter M are shown in Fig. 4. It is observed that when the compressibilities of the films are very high ($\nu_a<0.25$ and $\nu_b<0.25$), instabilities are not possible, whereas they undergo inhomogeneous deformations in the parametric space of $\nu_a>0.25$ and $\nu_b>0.25$. This is due to the fact that in a highly compressible film, the energy of homogeneous deformation is lower than that of inhomogeneous deformation. In the region $\nu_a>0.25$ and $\nu_b<0.25$, the greater the stiffness of the upper contactor film, the more is the area in the parametric space available for inhomogeneous deformations. Consider now the case when the substrate film is highly compressible ($\nu_a<0.25$), but the contactor film is less compressible ($\nu_b>0.25$). As the stiffness of the contactor film increases its incompressibility must also increase in order to cause instability. The limit $M\rightarrow 1$, denotes a completely rigid contactor film (the energy cost of deformation is infinite). In such a case, the instability is completely governed by the substrate film as is seen from Fig. 4. These results are in accordance with the results of a single film interacting with a rigid contactor [4].

The effect of the relative shear moduli on the wave number of instability for films with equal thicknesses is depicted in Fig. 5. For $\nu_a<\nu_b$, the value of hk_c decreases with an increase in M. For the case when the shear moduli of the system are also equal, i.e., $M=0.5$, it was already shown in the preceding section that $h_a k_c(\nu_a)<h_b k_c(\nu_b)$. Now, if the shear modulus of film b is only increased to make $M>0.5$, it follows that the wave number of instability of the film b increases, $[h_b k_c(M>0.5)>h_b k_c(M=0.5)]$, whereas, $h_a k_c$ remains unchanged (as μ_a is kept constant). The decrease in value of hk_c with increasing M indicates that the wave number of the two-film system does not reflect the change, as shown by the stiffer film b, but on the contrary decreases

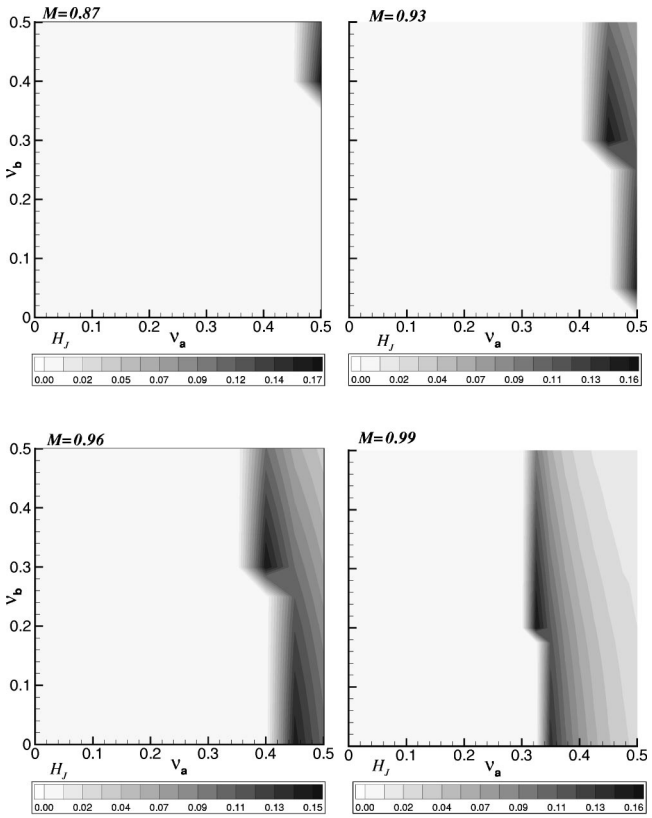

FIG. 11. The shaded regions in the figure denote the values of H_J at which jumps occur.

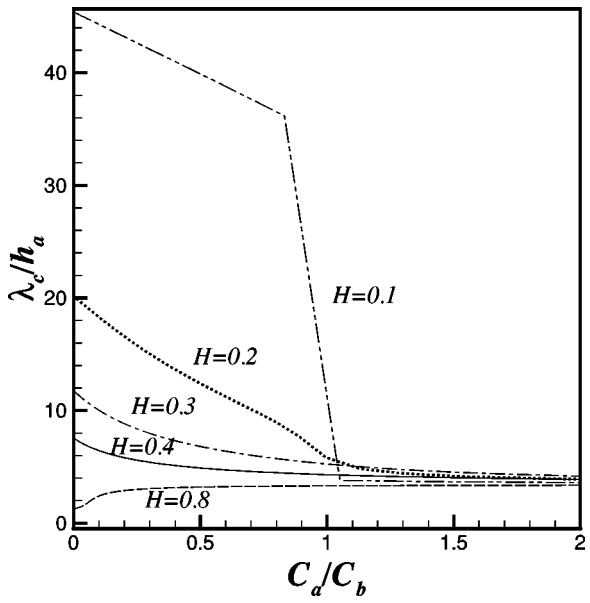

FIG. 12. The wavelength of instability as a function of the ratio of compliances when $\nu_a=0.45$ and $\nu_b=0.35$.

towards the wave number close to the compliant film *a*. This observation illustrates that the wavelength of instability of the system is determined to a much greater degree by the more compliant film. For a system with $\nu_a>\nu_b$, the critical wave number of instability increases with increase in *M*; this may be reasoned along the same lines as given above that the wavelength of instability is governed by the more compliant film. For films with equal thickness and equal Poisson's ratio, the wave number of instability, however, does not change with the relative shear moduli of the system. This is evident from the expression (36) by substituting $H=0.5$ and $\nu_a=\nu_b$.

It is seen from Fig. 5 that the nondimensional interaction stiffness $-Y_c/K_{eff}$ behaves in a similar fashion as hk_c, i.e., remains constant for $\nu_a=\nu_b$, increases for $\nu_a>\nu_b$, and decreases for $\nu_a<\nu_b$. But an increase or decrease in value of $-Y_c/K_{eff}$ does not imply an increase or decrease in $-Y_c$, because K_{eff}, in this case $M\mu_a/h_a$, is always increasing with an increase in *M*. Thus in the first two cases it is evident that $-Y_c$ of the system is increasing. It can be shown that the value of $-Y_c$ is increasing in the last case as well. For this purpose take a point in the parametric space $\nu_a=0.3$ and $\nu_b=0.4$, for $M=0.5$, $-Y_c/K_{eff}=3.96$ and for $M=0.8$, $-Y_c/K_{eff}=3.63$. The corresponding values of interaction stiffness are given as $-Y_c=1.98\mu_a/h_a$ and $-Y_c=2.91\mu_a/h_a$, respectively, showing that the value of the critical interaction stiffness is actually increasing with *M*. This result can be understood from the fact that as *M* increases, the effective stiffness of the system increases and the critical force required to cause inhomogeneous deformation also increases.

C. Films with equal shear moduli but different thicknesses

For the case when the shear moduli of the two films are equal, it is seen from Fig. 6 that films in the region $\nu_a<0.25$ and $\nu_b<0.25$ undergo homogeneous deformations, whereas films with Poisson's ratios $\nu_a>0.25$ and $\nu_b>0.25$ undergo inhomogeneous deformations, irrespective of their relative thicknesses.

In the parametric space where the substrate film is compressible compared to the contactor film ($\nu_a<0.25$ and $\nu_b>0.25$), as the thickness of the substrate film increases (*H* increases), the incompressibility of the contactor film should increase for surface roughening in the system to be possible. In the limit of $H\to 1$ (the case of a rigid contactor), surface instability is not possible when Poisson's ratio of the substrate film is less than 0.25, regardless of the compressibility of the contactor film. This result is also evident from Fig. 13, where it is seen that $hk_c=0$ for $\nu<0.25$.

Substitution of $M=0.5$ in Eq. (36) leads to an expression symmetric in *H* and ν. Thus, for a given value of *H* and ν_a the results are physically identical to that of $1-H$ and ν_b. This fact is evident from Fig. 6, where the demarcation lines for different values of *H* in the range $\nu_a<0.25, \nu_b>0.25$ are identical for the lines for $1-H$ in the range $\nu_a>0.25, \nu_b<0.25$.

The effective stiffness of a system with equal shear moduli is given by an expression $K_{eff}=(1-H)\mu_b/h_b$, wherein we assume that the thickness of the film *b* is kept constant and that of *a* is increased to have a higher value of *H*. It is evident that as the thickness of the substrate film increases (as *H* increases), the effective stiffness of the system decreases. The decrease in the value of hk_c with *H* as seen from Fig. 7 can be understood from the fact that as *H*

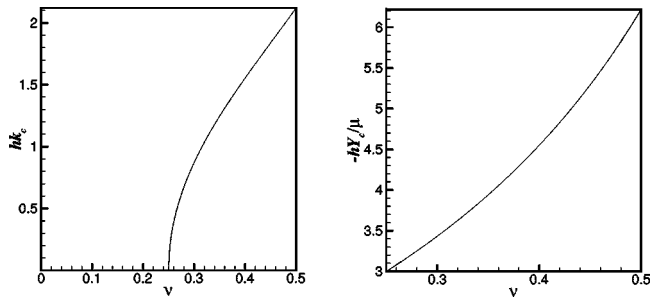

FIG. 13. Variation of bifurcation mode hk_c and critical interaction stiffness $-hY_c/\mu$ as a function of ν. The values of $-hY_c/\mu$ only in the range where $hk_c>0$ are shown.

increases the system becomes more compliant, implying a larger wavelength for the instabilities.

For a region in parametric space with $\nu_a \geqslant \nu_b$ it is seen that $-Y_c/K_{eff}$ increases with H and in a region with $\nu_a < \nu_b$ it is seen that $-Y_c/K_{eff}$ decreases with increasing H. However, an increase in $-Y_c/K_{eff}$ does not imply an increase in critical force parameter, since it has already been shown that K_{eff} decreases with decreasing H. Since the compliance of the system increases with increase in H, it is expected that $-Y_c$ should decrease with increasing H. The following values show that $-Y_c$, in fact, decreases with decreasing H for $\nu_a \geqslant \nu_b$: for $H=0.5$ and $\nu_a=0.4, \nu_b=0.3$, $-Y_c/K_{eff}=3.95 \rightarrow -Y_c=1.975\mu_b/h_b$, for $H=0.7$ and $\nu_a=0.4, \nu_b=0.3, -Y_c/K_{eff}=4.15 \rightarrow -Y_c=1.245\mu_b/h_b$; showing $-Y_c$ decreases with increase in H. These results again indicate that the instability is governed by the more compliant film.

D. Films with unequal thicknesses and moduli

The physics of instability in the general case can be understood based on the results of the previous cases. Comparison of Figs. 8 and 6 shows that the results for $M>0.5$ and different values of H are qualitatively similar to the case with $M=0.5$. Although the figures are quantitatively different (for example, the symmetry of the demarcation lines as in the case $M=0.5$, is absent in Fig. 8), the results can still be analyzed in a similar fashion as done for $M=0.5$.

However, for very small values of H and very high values of M, some qualitative changes in the results are observed. Very small values of H imply that the thickness of film b is much higher than film a, thus film b is the more compliant film which dictates the instability of the system. In Fig. 9, the horizontal demarcation lines for $0.5<M<0.9$ indicate that the system behaves as if film b is interacting with a rigid contactor and the effect of the presence of film a is negligible. However, for higher values of M ($M>0.9$), the shear modulus of film b becomes large than that of film a to the extent that the ratio μ_b/h_b exceeds μ_a/h_a, making film a the more compliant film. The transition of the horizontal line in the bifurcation diagram to the vertical one indicates that it is film a rather than film b that acts as the dominant film and governs the instability.

The values of $h_a k_c$ with $\nu_a=0.45, \nu_b=0.4$ as a function of H for different values of M are shown in Fig. 10. It is seen that for each value of M in the range $M \rightarrow 1$, there is a value of H (designated as H_J) where the value of $h_a k_c$ jumps from a higher value to a lower value on decreasing H. For $M=0.95$ at $H_J=0.095$, the value of $h_a k_c$ changes from ≈ 1.61 to ≈ 0.193. The latter can also be represented as $h_b k_c = 1.55$. Thus the instability mode of film a jumps from a higher value to a wave number that corresponds to the critical wave number of the film b, had it been interacting with a rigid contactor.

For given values of ν_a and ν_b the value of H_J decreases with increasing M. For example, when $\nu_a=0.45, \nu_b=0.4$, it is seen from Fig. 11 that $H_J|_{M=0.93}=0.129, H_J|_{M=0.99}=0.0215$. For $M \rightarrow 1$, film b moves towards the limit of a rigid contactor and for values of H much larger than zero film "a" is the more compliant film. However, if H is made close to zero, i.e, film a is made much thinner than film b, it is possible to make film a stiffer than film b and the instability will then be governed by film "b." The value of H at which this occurs is H_J and for all values of H smaller than this value, instability is governed by film b. Thus as the value of M increases the value of H_J must decrease to make this "jump" possible.

For a fixed value of M, now keeping ν_a fixed if ν_b is increased, the factor $2(1-\nu_b)/(1-2\nu_b)$ [of the term $(1-2\nu)h/2\mu(1-\nu)$, which designates the compliance C of a film] increases, increasing the stiffness of film b and making film a the compliant film. However, if the contactor-film thickness h_b is also increased, the stiffness of film b decreases, and may even become lesser than that of film a. When this happens the jump occurs, or film b becomes the new dominant film. This is evident from Fig. 11, where it is seen that as ν_b increases H_J value decreases to fulfill the condition for the jump.

E. Role of compliance of the films

All the above results underline the fact that the compliances of the films play an important role in determining the dominant film. This point can be further illustrated from Fig. 12. The figure depicts that when the compliances of the films are very different (C_a/C_b ratio quite greater than 1), the wavelength of the system is governed by the more compliant film (that is, film a in this case) for all values of H. The role reversal of the dominant film mainly occurs in the range of C_a/C_b varying from 0 to 1. The transit is smooth for higher values of H but for smaller values of H the change is abrupt close to the ratio of 1, which is designated as jump in the previous results.

V. CONCLUSION

The analysis of the surface instability of two compressible interacting elastic films reveals several interesting results. The analysis pursued here represents the most general case of instability in soft thin elastic films from which all of the previous results [3,20] can be obtained as various limiting cases, for example, a single film interacting with a rigid contactor, two interacting incompressible films, etc.

(1) Surface roughening of the film surfaces is possible

when the separation between the two films is below a critical distance, or, in other words, the attractive interaction force between the two films exceeds a critical value. The wavelength of the inhomogeneous periodic deformation is, however, independent of the precise nature of attractive interactions, but depends on the film thicknesses, ratio of shear moduli, and Poisson's ratios of the films.

(2) It is shown that the introduction of a second film in place of a rigid contactor makes the system more compliant. The critical force required to cause instabilities in a more compliant system is less compared to the case when a single film interacts with a rigid contactor. For example, it can be seen in Fig. 4 that the introduction of a contactor film causes surface instability in a compressible film, which is otherwise stable against inhomogeneous deformation.

(3) Irrespective of the shear moduli and thicknesses of the films highly compressible films (Poisson's ratio of both films less than 0.25) that are also highly compliant, deform homogeneously and jump in contact uniformly without any surface roughening. The same behavior was also observed in the case of a single elastic film interacting with a rigid contactor [3,4]. Thus, for almost all materials of interest ($\nu > 0.25$), surface roughening should occur readily below a critical separation.

(4) The compliance of a film is defined by $(1-2\nu)h/2\mu(1-\nu)$. The most important result found from the present analysis is that the properties of the more compliant film have a much greater influence on the wavelength of instability. When the compliances of the two films are very different, the wave number is a smooth function of the compliance ratio. However, when parameters are changed in the range $H \to 0, M \to 1$ such that the two compliances become similar, there is an abrupt change in the wave number of instability. On either side of this jump, however, the wavelength is governed largely by the properties of the more compliant film.

The above results presented are expected to be useful in the design and interpretation of important experiments related to cavitation, adhesion, and friction at soft interfaces.

ACKNOWLEDGMENTS

V.S. wishes to thank DST, India, for support of this work under the Fast Track Scheme. A.S. acknowledges the support of SAMTEL Center at IITK and MHRD.

APPENDIX A: TRACTION ALONG THE SURFACE OF AN ELASTIC FILM BONDED TO A SUBSTRATE WITH SINUSOIDAL SURFACE DEFORMATION

This section formulates the normal traction along the sinusoidally deformed surface of a film bonded to a rigid substrate. The system under consideration can be visualized from Fig. 1, when the top contactor is either very stiff or has a negligible thickness, and is subjected to the following boundary conditions:

$$u_1^{ai}(x_1,-h) = u_2^{ai}(x_1,-h) = 0,$$

$$u_2^{ai}(x_1,0) = \alpha\cos(kx_1), \quad \sigma_{12}^{ai}(x_1,0) = 0. \tag{A1}$$

The equilibrium equation of the system in terms of the displacements is given by the Navier's equation

$$(1-2\nu)u_{l,mm} + u_{m,ml} = 0. \tag{A2}$$

A general solution for the above set of differential equations, which anticipates a sinusoidally deformed surface, is given by

$$\begin{aligned} u_1^{ai}(x_1,x_2) &= -\frac{\alpha}{k}\{[B(3-4\nu)+k(A+Bx_2)]e^{kx_2} \\ &\quad +[D(3-4\nu)-k(C+Dx_2)]e^{-kx_2}\}\sin(kx_1), \\ u_2^{ai}(x_1,x_2) &= \alpha[(A+Bx_2)e^{kx_2}+(C+Dx_2)e^{-kx_2}]\cos(kx_1), \end{aligned} \tag{A3}$$

where the constants A, B, C, and D can be determined by substituting the boundary conditions (A1) in Eq. (A3). The solution yields

$$\begin{aligned} A &= \{-(kh+k^2h^2-2\nu kh)e^{kh}\cosh(kh) \\ &\quad +(2\nu-2+kh)[(3-4\nu)e^{kh}\cosh(kh) \\ &\quad +khe^{kh}\sinh(kh)]\} \\ &\quad /\{(\nu-1)[2(3-4\nu)\sinh(2kh)-4kh]\}, \\ B &= [(-2\nu+kh+1)e^{kh}\sinh(kh)-(2\nu-2+kh) \\ &\quad \times e^{kh}\cosh(kh)]/(\nu-1)[2(3-4\nu)\sinh(2kh)-4kh], \\ C &= 1-A, \\ D &= B-\frac{k}{2(\nu-1)}. \end{aligned} \tag{A4}$$

From these relations, the expression for the normal component of traction along the surface of the film can be derived as

$$\begin{aligned} \sigma_{22}^{ai}(x_1,0) &= \frac{2\mu}{(1-2\nu)}[\nu u_{1,1}+(1-\nu)u_{2,2}] \\ &= 2\mu[k\alpha\cos(kx_1)](A-C) \\ &\quad +2\mu(1-2\nu)\alpha\cos(kx_1)(B+D). \end{aligned} \tag{A5}$$

Replacement of the values of A, B, C, and D simplifies the expression to

$$\sigma_{22}^{ai}(x_1,0) = 2\mu S(kh,\nu)k\alpha\cos kx_1, \tag{A6}$$

where the function S is defined in Eq. (29).

APPENDIX B: ELASTIC ENERGY STORED PER UNIT LENGTH OF THE SYSTEM

The elastic energy stored in the film of length L is given by

$$\Pi_E = \int_V \frac{1}{2}\sigma_{lm}^{ai}\varepsilon_{lm}^{ai}dV = \int_V \frac{1}{2}\sigma_{lm}^{ai}u_{l,m}^{ai}dV$$

$$= \int_V \frac{1}{2}[\sigma_{lm}^{ai}u_l^{ai}]_m dV = \int_S \frac{1}{2}[\sigma_{lm}^{ai}]u_l^{ai}n_m dS$$

$$= \int_{top\text{-}interface} \frac{1}{2}[\sigma_{22}^{ai}]u_2^{ai}dS, \tag{B1}$$

surface integrals over all other interfaces are zero.

Thus assuming a surface profile of the form

$$u_2^{ai}(x_1,0) = \alpha\cos(kx_1), \tag{B2}$$

we get the stored elastic energy per unit length of the film in the form

$$\Pi_E = \frac{1}{L}\int_0^L \frac{1}{2}\sigma_{22}^{ai}(x_1,0)u_2^{ai}(x_1,0)dx_1$$

$$= \frac{1}{L}\int_0^L \frac{1}{2}[2\mu S(kh,\nu)k\alpha\cos(kx_1)]\alpha\cos(kx_1)dx_1$$

$$= \frac{\mu}{L}S(kh,\nu)k\alpha^2 L = \alpha^2 k\mu S(kh,\nu). \tag{B3}$$

The variation of the wave number that minimizes Eq. (B3), with the Poisson's ratio of the film is shown in Fig. 13. In the same figure, the corresponding critical interaction stiffness is also shown. The expression for Y_c can be obtained from Eq. (30) by setting $\mu_b \gg \mu_a$ or $h_a \gg h_b$.

For the interacting two-film system described in the text, the total elastic energy stored per unit length of the films is the sum of the energies stored in the individual films and is given by the expression

$$\Pi_E = \alpha^2 k\mu_a S(h_a k,\nu_a) + \beta^2 k\mu_b S(h_b k,\nu_b). \tag{B4}$$

[1] A. Ghatak, M.K. Chaudhury, V. Shenoy, and A. Sharma, Phys. Rev. Lett. **85**, 4329 (2000).
[2] W. Mönch and S. Herminghaus, Europhys. Lett. **53**, 525 (2001).
[3] V. Shenoy and A. Sharma, Phys. Rev. Lett. **86**, 119 (2001).
[4] V. Shenoy and A. Sharma, J. Mech. Phys. Solids **50**, 1155 (2002).
[5] K.R. Shull, C.M. Flanigan, and A.J. Crosby, Phys. Rev. Lett. **84**, 3057 (2000).
[6] S. Herminghaus, K. Jacobs, K. Mecke, J. Bischof, A. Fery, M. Ibn-Elhaj, and S. Schlagowski, Science **282**, 916 (1998).
[7] A. Sharma and R. Khanna, Phys. Rev. Lett. **81**, 3463 (1998).
[8] G. Reiter, R. Khanna, and A. Sharma, Phys. Rev. Lett. **85**, 1432 (2000).
[9] E. Schäffer, T. Thurn-Albrecht, T.P. Russel, and U. Steiner, Nature (London) **403**, 874 (2000).
[10] R.J. Asaro and W.A. Tiller, Metall. Trans. **3**, 1789 (1972).
[11] M. Grinfeld, J. Nonlinear Sci. **3**, 35 (1993).
[12] D. Srolovitz, Acta Metall. **37**, 621 (1989).
[13] J.C. Ramirez, Int. J. Solids Struct. **25**, 579 (1989).
[14] D.A. Kessler, Nature (London) **413**, 260 (2001).
[15] L. Kogan, C.-Y. Hui, and A. Ruina, Macromolecules **29**, 4090 (1996).
[16] M. Newby, B.Z. Chaudhury, and H. Brown, Science **269**, 1407 (1995).
[17] C. Gui, M. Elwenspoek, N. Tas, and J.G.E. Gardeniers, J. Appl. Phys. **85**, 7448 (1999).
[18] R. Budakian and S.J. Putterman, e-print cond-mat/0203075.
[19] C. Ru, J. Appl. Phys. **90**, 6098 (2001).
[20] V. Shenoy and A. Sharma, Langmuir **18**, 2216 (2002).